LECTURE 9: Application of Landauer-Büttiker formula to quantum interference effects in electronic transport

1° Quantum interference in two-slit example from elementary QM

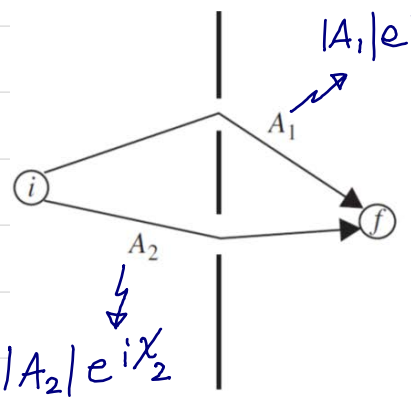

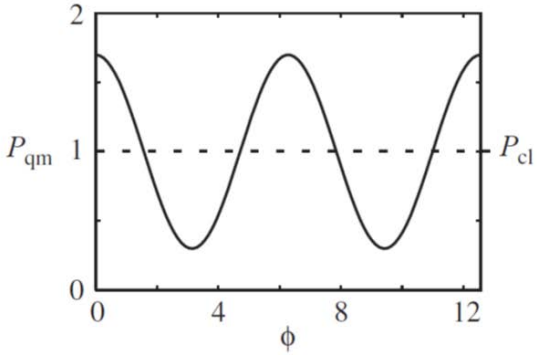

→ $P_{QM} > P_{cl}$ for $\cos\phi > 0$ is constructive interference

→ for $P_1 = P_2$ destructive interference $P_{QM} = 0$ at $\chi = \pi + 2\pi n$

$$P_{cl} = P_1 + P_2 = |A_1|^2 + |A_2|^2$$

↳ classical probability

$$P_{QM} = |A_1 + A_2|^2 = |A_1|^2 + |A_2|^2 + A_1 A_2^* + A_1^* A_2$$

↳ quantum probability

$$= P_{cl} + 2\,\mathrm{Re}\left(A_1 A_2^*\right)$$

$$= P_{cl} + 2\sqrt{P_1 P_2}\cos\chi \,, \quad \chi = \chi_1 - \chi_2$$

$\chi \neq 0$ is generated by displacing ① or ② with respect to the slits

2° Aharonov-Bohm ring

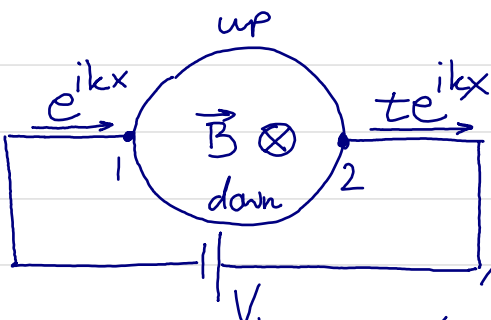

$$t_{21}^u = t_{21} e^{i\chi_1}, \quad t_{21}^d = t_{21} e^{i\chi_2}$$

$$\chi_1 = \frac{e}{\hbar}\int \vec{A}\cdot d\vec{r} \qquad \chi_2 = \frac{e}{\hbar}\int \vec{A}\cdot d\vec{r}$$

$$\chi = \chi_1 - \chi_2 = \frac{e}{\hbar}\oint \vec{A}\cdot d\vec{r} = \int \vec{B}\cdot d\vec{S} = 2\pi\,\Phi/\Phi_0 \,; \qquad \Phi_0 = h/e$$

$$t = t_{21}^u + t_{21}^d = t_{21}(E)\, e^{\frac{i(\chi_1+\chi_2)}{2}}\left[e^{i\chi/2} + e^{-i\chi/2}\right] \Rightarrow T = |t|^2 = |t_{21}^u + t_{21}^d|^2$$

$$= 2T_{21} + 2T_{21}\cos\chi$$

$$G = \frac{2e^2}{h}T \longrightarrow 0$$ ↳ destructive interference when $\chi = \pi + 2\pi n$, $n = 0, \pm 1, \pm 2, \ldots$

PHYSICAL REVIEW B 77, 085413 (2008)

Observation of Aharonov-Bohm conductance oscillations in a graphene ring

Saverio Russo,* Jeroen B. Oostinga, Dominique Wehenkel, Hubert B. Heersche, Samira Shams Sobhani, Lieven M. K. Vandersypen, and Alberto F. Morpurgo†

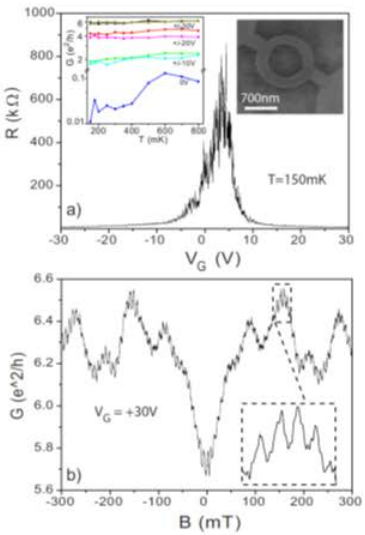

FIG. 1. (Color online) (a) The main panel shows the two-probe measurement of the ring resistance versus back gate voltage at $T=150$ mK. The charge neutrality point is at +4 V. Left inset: temperature dependence of the conductance measured for different values of gate voltage. Right inset: scanning electron microscopy image of a ring-shaped device etched in graphene similar to the one used in our measurements. (b) Magnetoconductance of the graphene ring measured at $T=150$ mK and $V_G=+30$ V. On top of the aperiodic conductance fluctuations, periodic oscillations are clearly visible as also highlighted in the inset.

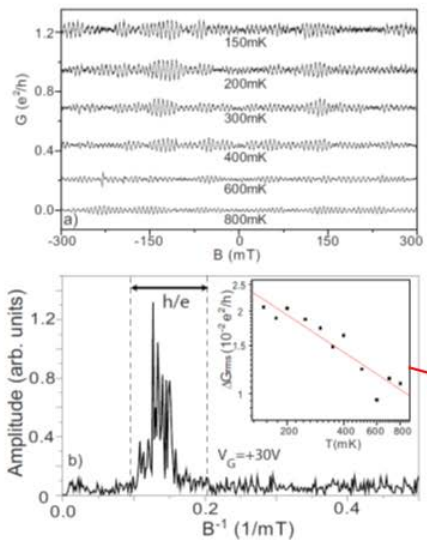

FIG. 2. (Color online) (a) Aharonov-Bohm conductance oscillations measured at $V_G=+30$ V for different temperatures (curves are offset for clarity). (b) Fourier spectrum of the oscillations measured at $T=150$ mK shown in panel (a). The vertical dashed lines indicate the expected position of the h/e peak, as determined from the inner and outer radii of the ring. In the inset: temperature dependence of the root mean squared amplitude of the AB conductance oscillations, obtained from the measurements shown in panel (a).

calization of electron states. To estimate the mobility μ of charge carriers, we use the value of the conductance per square measured at high gate voltage. With the density of charge carriers being determined from the known capacitance to the gate (i.e., $G_\square = ne\mu = \varepsilon_0\varepsilon_r e\mu V_G/d$), we obtain $\mu = 6000\ \mathrm{cm^2/V\,s}$, essentially independent of V_G for $V_G > 10$ V and $V_G < -10$ V. The diffusion constant is estimated from the Einstein relation $\sigma = \nu e^2 D$, where σ is the measured conductivity and ν the density of states at the Fermi level, which for graphene is given by $\nu(\varepsilon_F) = g_s g_v 2\pi|\varepsilon_F|/(h^2 v_F^2)$.[15] Here, $g_v=2$ and $g_s=2$ account for the valley and spin degeneracies, $v_F = 10^6$ m/s is the Fermi velocity, and the value of ε_F is determined by equating the expression for the charge density $n(\varepsilon_F) = g_s g_v \pi \varepsilon_F^2/(h^2 v_F^2)$ to the value determined by the gate voltage. We obtain $D = 0.06\ \mathrm{m^2/s}$, not far from the value of diffusion constant that is estimated assuming diffusive scattering at the ribbon edges ($D = W v_F = 0.15\ \mathrm{m^2/s}$, with W the width of the ribbon). With this value of the diffusion constant, we obtain a Thouless energy for the ring of $E_{\mathrm{Th}} = \hbar D/L^2 = 10\ \mu$eV ($L$ is the ring circumference), which is slightly smaller than the lowest temperature ($T=150$ mK) at which the measurements have been performed.

metal rings, is due to thermal averaging of the h/e oscillations $[\delta G_{AB}\alpha(E_{\mathrm{Th}}/k_B T)^{1/2}\exp(-\pi r/L_\phi(T))$, where r is the radius of the ring].[7] It is expected for temperature values larger than the Thouless energy (which is the case here), if the phase coherence $L_\varphi = (D\tau_\varphi)^{1/2}$ length is longer than the arms of the ring. Indeed, with the value of diffusion constant given above and taking for the phase coherence time values estimated in the literature (away from the charge neutrality region $\tau_\phi \sim 0.1$ ns at $T=1$ K, increasing roughly linearly with decreasing T),[16] we find that in our ring also this condition is satisfied. A similar $T^{-1/2}$ dependence was observed for all gate voltages at which the AB oscillation amplitude was sufficiently large to be accurately measured.

3° Tunneling in double barrier junction

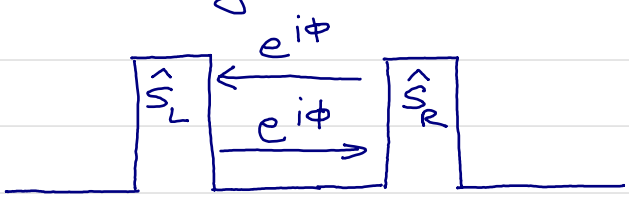

$\hat{S}_L$, $\hat{S}_R$ are 2×2 scattering matrices

$$d\Phi/dE = \int_{t_1}^{t_2} \frac{dt}{\hbar} = \frac{\tau}{\hbar}$$

↳ dynamical phase

τ is time of flight between two points in space at energy E

$$\hat{S}_L = \begin{pmatrix} r_L & t_L' \\ t_L & r_L' \end{pmatrix} \qquad \hat{S}_R = \begin{pmatrix} r_R & t_R' \\ t_R & r_R' \end{pmatrix}$$

$T_L = |t_L|^2$, $R_L = 1 - T_L$

$T_R = |t_R|^2$, $R_R = 1 - T_R$

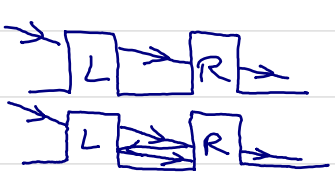

$$A_1 = t_L e^{i\Phi} t_R$$

$$A_2 = t_L r_L' r_R t_R e^{i3\Phi}$$

$$\Rightarrow A_m = t_L t_R (r_L' r_R)^{m-1} \cdot e^{(2m-1)\Phi}$$

→ total probability amplitude to propagate from left to right:

$$t = \sum_{m=1}^{\infty} A_m = t_L t_R e^{i\Phi} \sum_{m=0}^{\infty} \left(r_L' r_R e^{2i\Phi} \right)^m$$

$$= \frac{t_L t_R}{1 - r_L' r_R e^{2i\Phi}}$$

$$T = |t|^2 = \frac{T_L T_R}{1 + R_L R_R - 2 R_L R_R \cos 2\chi}$$

is periodic function of energy with period $2\pi\hbar/\tau$

$$2\chi = 2\Phi + \arg(r_L' r_R)$$

↳ dynamical phase collected during round trip from left to right barrier and back

$$T_{min} = \frac{T_L T_R}{(1 + \sqrt{R_L R_R})^2} < T(\chi) < \frac{T_L T_R}{(1 - \sqrt{R_L R_R})^2} = T_{max}$$

$$T_{L,R} \ll 1 \Rightarrow \begin{cases} T_{min} \approx T_L \cdot T_R \ll 1 \\ T_{max} = \dfrac{4 T_L T_R}{(T_L + T_R)^2} \end{cases}$$ can be even 1 for $T_L = T_R$

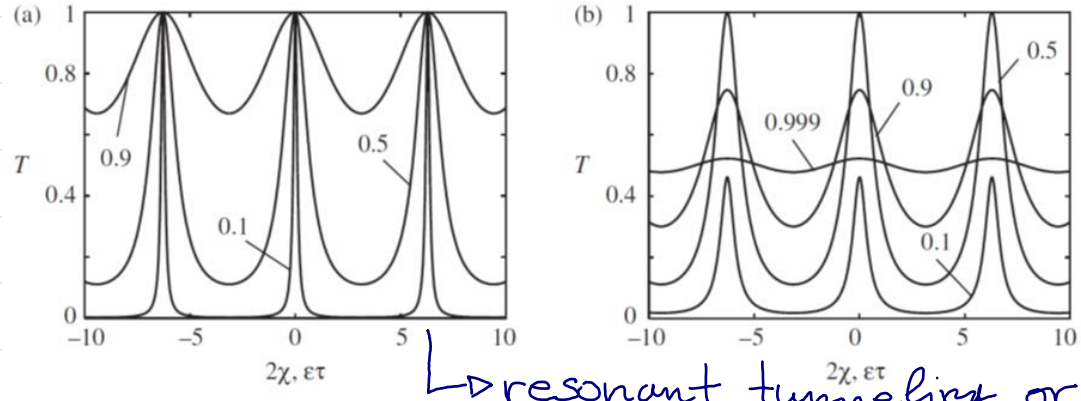

Transmission via double junction versus phase shift or energy. (a) Symmetric scatterers with $T_1 = T_2$ corresponding to the curve labels. The maximum transmission is always 1 in this case. (b) Non-symmetric scatterers, $T_1 = 0.5$, and T_2 corresponds to the curve labels. The narrow transmission resonances for $T_{1,2} \ll 1$ indicate formation of discrete energy levels at corresponding energies.

↳ resonant tunneling or Fabry-Perot resonances

$$T_{ce} = \sum_{m=0}^{\infty} |A_m|^2 = T_L T_R \sum_{m=0}^{\infty} (R_L R_R)^m = \frac{T_L T_R}{1 - R_L R_R}$$

is independent of phase shift χ or energy

$$T_{L,R} \ll 1 \Rightarrow G_{ce} = \frac{2e^2}{h} T_{ce} = \frac{G_L G_R}{G_L + G_R}$$

$$\Updownarrow$$

$$1/G_{ce} = 1/G_L + 1/G_R$$

Ohm law for two resistors in series

→ anything beyond Ohm law, such as resonant tunneling, cannot be described by classical transport and, therefore, has to be associated with quantum interference

4° Strong and weak localization

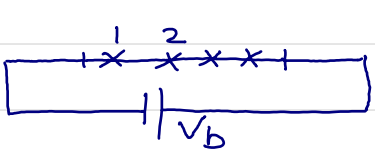

$$g_{12} = \left\langle \frac{1-T}{T} \right\rangle_{\text{over } \chi} = \int_0^{2\pi} \frac{d\chi}{2\pi} \frac{1 + R_1 R_2 - T_1 T_2 - 2\sqrt{R_1 R_2}\cos 2\chi}{T_1 T_2}$$

↳ 4-terminal resistance as the property of two barriers without the semi-infinite leads where we remove unit $h/2e^2$

→ averaging over χ is justified by having pairs of scatterers at different distances

$$g_1 = \frac{R_1}{T_1} \; ; \; g_2 = \frac{R_2}{T_2}$$ → resistances of individual scatterers

$$\rho_{12} = \frac{1 + R_1 R_2 - T_1 T_2}{T_1 T_2} = \frac{R_1 + R_2}{T_1 T_2} = \frac{R_1}{T_1} + \frac{R_2}{T_2} + \frac{2 R_1 R_2}{T_1 T_2}$$

$$= \rho_1 + \rho_2 + \underbrace{2\rho_1\rho_2}_{\text{extra term when compared to classical Ohm law}}$$

$$\rho(L + \Delta L) = \rho(L) + [1 + 2\rho(L)]\frac{\Delta L}{\lambda}$$

↑ resistance of nanowire of length $L + \Delta L$

↑ ρ_1

$\rho_2 = \frac{\Delta L}{\lambda}$ is added resistor in series

$$\Delta L \to 0 \Rightarrow \frac{\rho(L+\Delta L) - \rho(L)}{\Delta L} = \frac{1 + 2\rho(L)}{\lambda}$$

$$\underbrace{\rho(L) = \frac{1}{2}\left(e^{2L/\lambda} - 1\right)}_{\text{Anderson localization}} \qquad L \ll \lambda$$

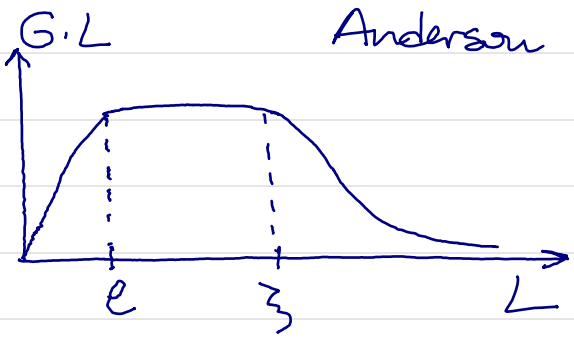

$$\rho(L) = \frac{L}{\lambda}$$

so λ is of the order of mean free path ℓ by comparing to Drude formula

↠ expanding $\rho(L)$ to second order:

$$\rho(L) = \frac{L}{\lambda} + \left(\frac{L}{\lambda}\right)^2 = \rho_{cl} + \Delta\rho$$

$$\frac{G}{2e^2/h} \approx \frac{1}{\rho_{cl} + \Delta\rho} \approx \frac{1}{\rho_{cl}} - \frac{\Delta\rho}{\rho_{cl}^2} = \frac{1}{\rho_{cl}} - 1$$

↠ weak localization reduces conductance of phase-coherent conductor by $\Delta G_{WL} \approx 2e^2/h$

→ localization length can be estimated by demanding that for $L = \xi$:

$$\frac{G_{ee}(L=\xi)}{2e^2/h} = \frac{N_{ch} \cdot \ell}{\xi} \approx 1 \quad \Rightarrow \quad \xi \approx N_{ch} \cdot \ell \approx \frac{k_F^2 A}{4\pi} \cdot \ell$$

$$G_{ee} = \frac{2e^2}{h} \cdot \frac{k_F^2 A}{4\pi} \frac{4}{3} \frac{\ell}{L}$$

→ for 100 nm × 100 nm wire with $\sim 10^5$ modes and $\ell \sim 10$ nm $\Rightarrow \xi \sim 1$ mm $\gg L_\phi$

5° Universal conductance fluctuations (UCF)

Experiment:

ARTICLE

DOI: 10.1038/s42005-017-0001-4 OPEN

Exotic multifractal conductance fluctuations in graphene

Kazi Rafsanjani Amin[1], Samriddhi Sankar Ray[2], Nairita Pal[1], Rahul Pandit[1] & Aveek Bid[1]

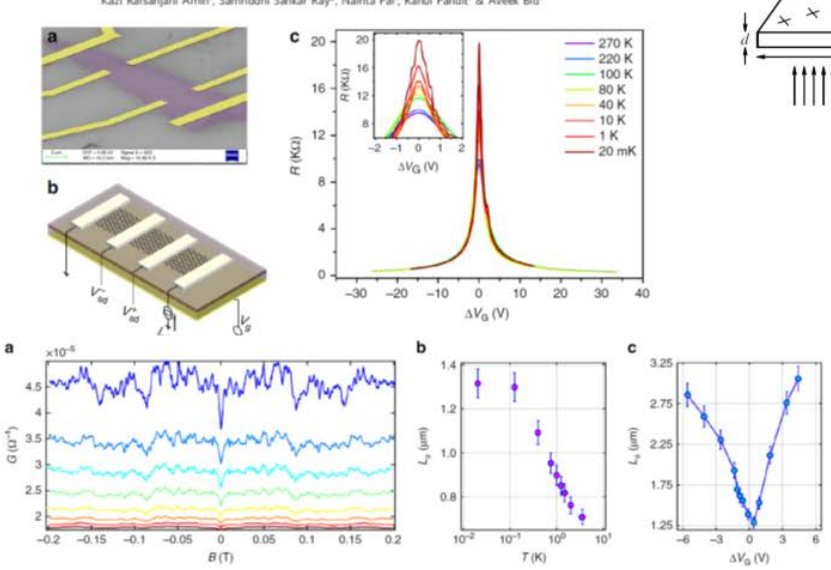

Fig. 2 UCF in graphene. **a** Illustrative plots of the magnetoconductance G versus the magnetic field B measured at 0.02, 0.05, 0.075, 0.10, 0.20, 0.50, 1.00, and 2.00 K (from top to bottom—curves for different temperatures have been shifted vertically for clarity). The data shown here are from the device G28M6 measured close to the Dirac point ($\Delta V_G = 0.2$ V). **b** Plot of the phase-coherence length L_ϕ versus the temperature T extracted from the UCF measured at $\Delta V_G = 0.2$ V. **c** Plot of L_ϕ versus ΔV_G, extracted from the UCF measured at $T = 20$ mK. The error-bars in **b**, **c** represent the standard deviation in L_ϕ

Theory & Computation:

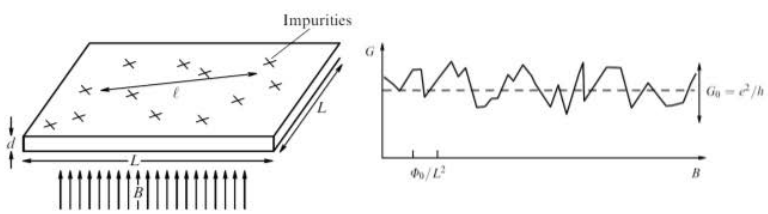

PHYSICAL REVIEW B, VOLUME 63, 020201(R)

Resistivity of a metal between the Boltzmann transport regime and the Anderson transition

Branislav K. Nikolić* and Philip B. Allen

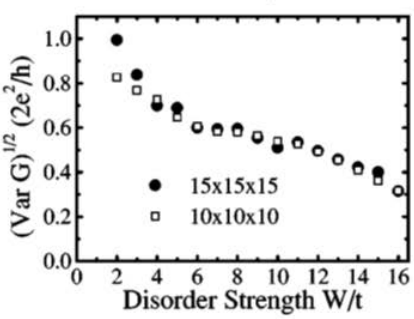

FIG. 3. The conductance fluctuations ($\Delta G = \sqrt{\mathrm{Var}\, G}$ at $E_F = 0$) from weak to strong scattering regime in the disordered cubic samples $10\times10\times10$ and $15\times15\times15$.

$$\Delta G = \sqrt{\langle (G - \langle G \rangle_{imp})^2 \rangle_{imp}} \approx e^2/h$$

→ is universal or independent of disorder details!

↳ average is performed over all possible impurity configurations

$$\langle G \rangle_{imp} = \sigma \frac{A}{L} = \sigma \frac{dL}{L}$$

in the semi-classical diffusive or Ohmic regime

⇝ relative fluctuation: $\frac{\Delta G}{\langle G \rangle_{imp}} \approx \frac{e^2}{h} \frac{1}{d\sigma}$

is independent of conductor size L, which is surprising because one naively expects that as $L \to \infty$ conductance is self-averaging (like quantities in statistical mechanics) and relative fluctuation should decrease

⇝ distribution function of transport and equilibrium quantities in quantum-coherent nanostructures is very far away from Gaussian with long tails due to rare events, so it cannot be described by just two parameters $\langle O \rangle_{imp}$ and ΔO:

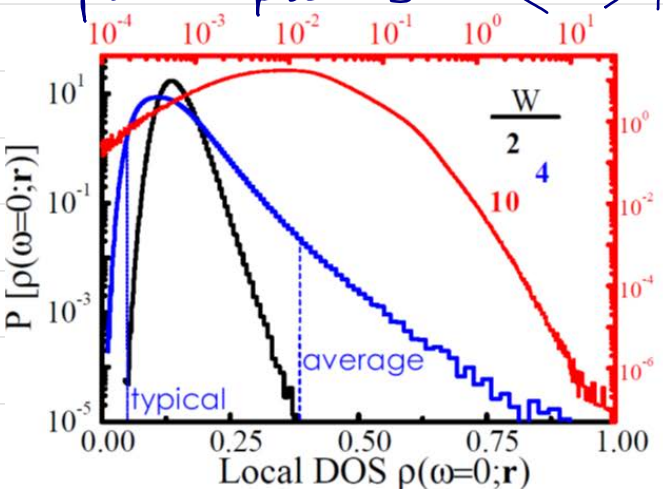

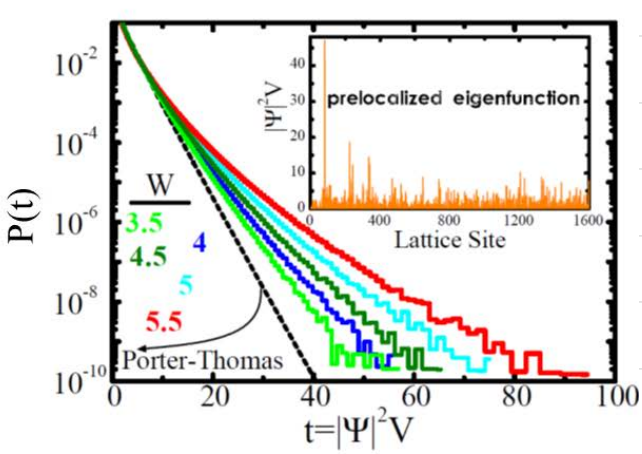

- instead of fabricating many samples with different impurity configurations, we can also focus on a single sample and change magnetic field

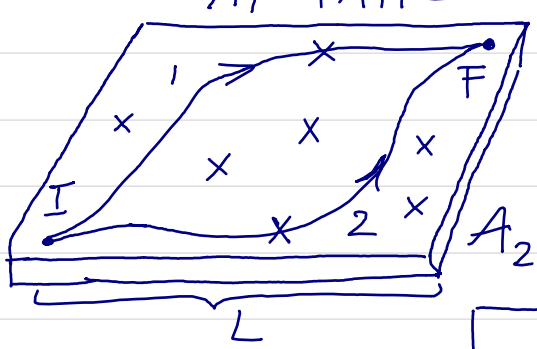

$A_1 = |A_1| e^{i\chi_1}$

$A_2 = |A_2| e^{i\chi_2}$

$\langle P_{I\to F} \rangle_{imp} = \langle |A_1|^2 + |A_2|^2 \rangle_{imp}$

$\underbrace{\langle 2|A_1||A_2|\cos\chi \rangle_{imp}}_{=0}$

vanish due to averaging over the random phase

neglect WL

$\langle P^2_{I\to F} \rangle_{imp} \propto \langle (|A_1|^2 + |A_2|^2)^2 \rangle_{imp}$

$+ \langle 2|A_1|^2 |A_2|^2 \rangle_{imp} =$

$= \langle P_{I\to F} \rangle^2_{imp} + \langle 2P_1 P_2 \rangle_{imp}$

$\Delta P_{I\to F} = \sqrt{\langle (P_{I\to F} - \langle P_{I\to F} \rangle_{imp})^2 \rangle_{imp}}$

$= \sqrt{\langle 2P_1 P_2 \rangle_{imp}}$

→ as we change $\vec{B}$, relative phase between all paths changes, so that conductance changes accordingly

WEAK LOCALIZATION IN PICTURES

the exception is the contribution from paths, or segment of paths, repeating the motion backward and contributing to weak localization

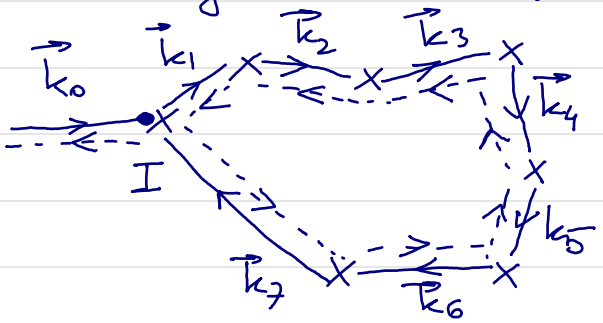

$\langle P_{a\to a} \rangle_{imp} = \langle |A_1|^2 + |A_2|^2 \rangle_{imp}$

probability to return to point I $= \underbrace{4|A_1|^2}_{\text{quantum}} > \underbrace{2|A_1|^2}_{\text{classical}} + \langle 2|A_1||A_2| \rangle_{imp}$